Charge States of a Helium Beam in Hydrogen, Helium, Air, and Argon*

ELIAS SNITZER
Department of Physics and Institute for Nuclear Studies, University of Chicago, Chicago, Illinois
(Received November 28, 1952)

Measurements have been made of the fractions of a helium beam in the He^0, He^+, and He^{++} charge states in the energy range of 100 kev to 480 kev for beams in hydrogen, helium, air, and argon. For the four gases, the He^0 and He^+ components are equal for helium energies of 148 kev, 145 kev, 98 kev, and 115 kev, respectively. The ratios of the electron loss to electron capture cross sections between He^+ and He^{++} fitted a simple power dependence of $(\sigma_l/\sigma_c) \propto V^m$, where V is the velocity of the helium in the beam and m equals 6.1, 5.1, 5.2, and 6.3, respectively, for the four gases studied. For electron capture and electron loss between He^0 and He^+ the exponent m varies from 2.6, 2.0, 2.8, and 3.4 at 100 kev to 4.0, 4.0, 4.3, and 5.1 at 450 kev.

I. INTRODUCTION

WHEN a high energy ion beam passes through matter, it not only loses energy by exciting and ionizing the particles of the matter through which it traverses, but it also undergoes a process of charge exchange by capturing from, or losing electrons to, the matter being traversed. For singly charged ions such as protons and He^+, charge exchange between the neutral and singly ionized states does not become significant until the ion has been slowed down to where its velocity is comparable to the velocity of the outer electrons in the matter being traversed. The velocities at which exchange between multiply charged states is significant are higher. This paper relates the work done in determining the fractions of a helium beam in its three charge states, He^0, He^+, and He^{++}, for energies varying from 100 kev to 480 kev when the beam passes through hydrogen, helium, air, and argon.

The problem of the capture and loss of electrons by moving ions has been of interest since the discovery of canal rays. The earlier work has been reviewed by Rüchardt.[1] Singly charged alpha-particles were discovered by Henderson[2] in 1922. The experiments of Rutherford[3] on charge exchange for helium covered energies from 0.65 Mev to 6.78 Mev, and a considerable amount of work[4] on various ions for energies up to 100 kev has been reported, but no work has been done on helium in the interesting region of 100 kev to 500 kev, where most of the helium is in the single charged state. Recently, experiments have been carried out to determine the capture and loss cross sections for protons of energies from 20 kev to 400 kev.[5–9]

Besides the value in filling the gap for helium between Rutherford's high energy experiments and the work done up to 100 kev,[5,10–14] this problem is also of interest on other accounts. Accurate information regarding the fraction of a beam in a particular charge state is useful in experiments where the response of detectors and other apparatus is charge dependent. The process is important in the slowing down of fission fragments, for capture and loss of electrons is significant throughout the entire path of the fragment because of the large initial charge. The average charge of the ions in a beam affects the rate of energy loss by ionization and excitation of the medium, as indicated by the Bethe-Bloch formula. Also, the process of charge exchange itself contributes to the slowing down of the ion, for a cycle of capture and loss of an electron results in the creation of one ion pair.

II. DESCRIPTION OF APPARATUS

A. General

The singly ionized helium beam was produced by the University of Chicago 500 000-volt kevatron (Cockcroft-Walton generator). The beam was selected by a magnet H_1, which caused the accelerated He^+ ions to enter a port which made a 15° angle with the axis of the kevatron. The beam then entered the 74-cm long pipe A filled with the target gas. After passing through the pipe and undergoing charge exchange, the beam entered the evacuated magnetic deflection chamber B, where it was separated into its charged states. To maintain the gas pressure in the pipe without interfering either with the vacuum of the kevatron or the vacuum in the magnetic deflection chamber, one stage of differential pumping was used on either side of the pipe containing the gas. Differential pumping instead of a foil was used at the entrance to the pipe so as to make the apparatus durable and to avoid the difficulty of making and installing foils. Differential pumping had the additional advantage that it avoided difficulties

* This work was supported in part by a grant from the U. S. Atomic Energy Commission.

[1] E. Rüchardt, *Handbuch der Physik* (J. Springer, Berlin, 1933), Vol. 22, No. 2, p. 103.
[2] G. H. Henderson, Proc. Roy. Soc. (London) **102**, 496 (1922).
[3] E. Rutherford, Phil. Mag. **47**, 277 (1924).
[4] A summary of the work done on protons, helium, and other ions is given in H. S. W. Massey and E. H. S. Burhop, *Electronic and Ionic Impact Phenomena* (Oxford University Press, London, 1952), Chap. VIII, Sec. 6.
[5] J. P. Keene, Phil. Mag. **40**, 369 (1949).
[6] T. Hall, Phys. Rev. **79**, 504 (1949).
[7] J. H. Montague, Phys. Rev. **81**, 1026 (1951).
[8] F. L. Ribe, Phys. Rev. **83**, 1217 (1951).
[9] H. Kanner, Phys. Rev. **84**, 1211 (1951).
[10] P. Rudnick, Phys. Rev. **38**, 1342 (1931).
[11] R. A. Smith, Proc. Cambridge Phil. Soc. **30**, 514 (1934).
[12] A. Rostagni, Nuovo cimento **12**, 134 (1935).
[13] F. Wolf, Ann. Physik **30**, 313 (1937).
[14] H. Meyer, Ann. Physik **37**, 69 (1940).

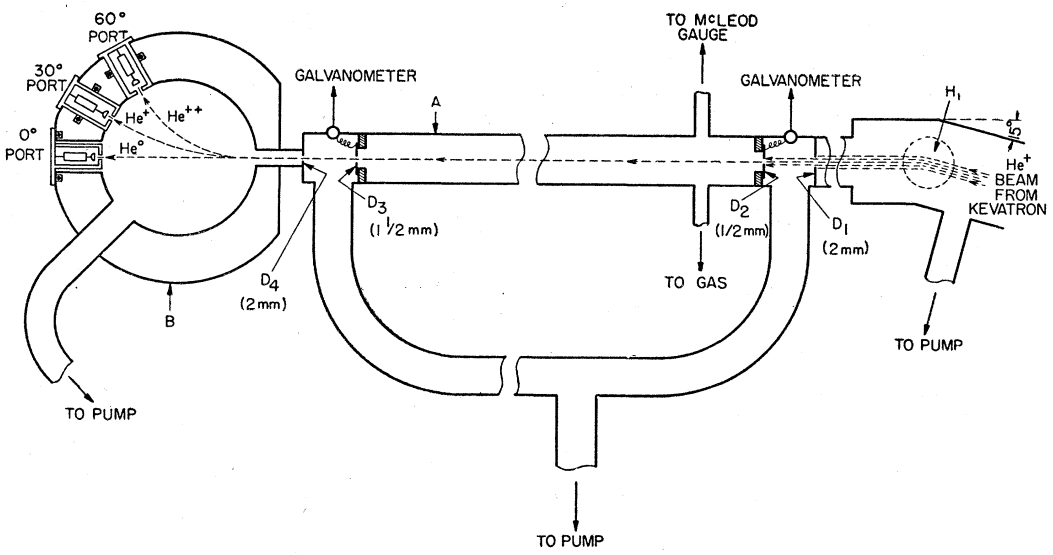

FIG. 1. Schematic drawing of the apparatus.

associated with determining the exact amount of slowing down of the beam as a result of passing through a foil. Of course, a foil could not be used at the emergent end of the pipe for the foil itself would have produced charge exchange. Figure 1 is a schematic drawing of the apparatus.

The energy of the beam particles was measured by the current drain through a resistor stack of 10^{10} ohms placed between the high voltage end of the kevatron and ground.

The pressure in the pipe was measured by a McLeod gauge. Pressures up to 8×10^{-2} mm of mercury were used in the pipe, but such a pressure did not cause the pressure in the magnetic deflection chamber to exceed 10^{-4} mm of mercury. The differential pumping sections were one inch long with two short lengths of $\frac{1}{2}$ in. i.d. tubing leading into the 2 in. i.d. tubing connecting to the vacuum pump.

The diameters of the holes through which the beam passed in entering and leaving the pipe are indicated in Fig. 1. Diaphragm D_2 was electrically insulated from the rest of the apparatus and connected to a galvanometer in order to use the current it collected as a monitor. Diaphragm D_3 was mounted behind another diaphragm with a $\frac{1}{4}$-in. hole and insulated from it. This arrangement greatly assisted alignment of the apparatus, for, when charge was collected on diaphragm D_3, the beam was no more than $\frac{1}{8}$ in. off from the center of D_3. The distance from D_2 to D_3 was 74 cm. The holes in D_1, D_2, D_3, and D_4 were aligned to within 0.005 in.

Except for one change, the magnetic deflection chamber and the magnet to provide its field were the same as used by Montague,[7] Ribe, and Kanner, and as described in detail by Montague. The change consisted of installing another port at 30° with respect to the incident beam direction. The magnet was water cooled. A dc motor-generator set rated at 220 volts and 6 amps activated the magnet. The output of the motor-generator set was controlled by a variable resistor in the self-excited shunt field of the generator.

B. The Detectors

The detectors each consisted of a thermistor Th_d enclosed in a nickel foil. (Figure 2 is a sketch of one of the detectors.) When the beam struck the foil the resultant heating of the foil and thermistor was measured by the change in resistance of the thermistor. The thermistors used were the type 27A thermistors manufactured by Western Electric.[15] These thermistors are beads of about $\frac{1}{2}$ mm in diameter with 0.001-in. nickel wire leads. The thermistor was enclosed in a cylindrical sheath of 0.001-in. thick nickel foil. The side of the cylindrical sheath facing the beam was flattened so that the entire beam struck the nickel surface perpendicularly. The flattened side of the sheath facing the beam was 5 mm high and 3 mm wide. Knife edges placed $\frac{1}{32}$ in. in front of the sheath stopped down the area exposed to the beam to 4 mm$\times2\frac{1}{2}$ mm. In this way, all the beam that entered the detector could hit only the nickel foil.

The nickel sheath was insulated from the thermistor by building up two globules G of glyptal paint on the wire leads on either side of the thermistor bead and having the nickel sheath rest on the hardened glyptal. The sheath was insulated from the thermistor so that the thermistor bead would not be electrically shorted out. Also, by this arrangement the sheath could be used to measure the charge collected, thus assisting in the alignment of the system by giving a rapid electrical response when the beam struck the detector.

The thermistor and sheath were mounted by solder-

[15] Becker, Green, and Pearson, Elec. Eng. **65**, 711 (1946).

ing the leads from the thermistor to 0.008-in. thick nickel wires that were screwed fast to a piece of Lucite enclosed in the brass housing of the detector.

In addition to the detecting thermistor, another thermistor with approximately the same characteristics as the first was enclosed in the same housing in order to make possible the rapid and accurate reading of the ambient temperature. The additional thermistor Th_a was placed $\frac{1}{2}$ in. from the sheath of the detector thermistor, and out of sight from it so that the sheath could not radiate heat directly to it.

Leads from the thermistors and sheath were brought out through vacuum tight insulators at the base of the detector housing.

The geometry of all three detectors was alike. The detector in the 0° port was placed in an adjustable mounting which made possible adjustment in the position of the detector with respect to the beam. The 30° and 60° ports did not have such adjustable mountings, since the positions of the He^+ and He^{++} beams could easily be adjusted by the magnetic field.

III. EXPERIMENTAL PROCEDURE

The positioning of the beam so that it would pass through the differential pumping sections and enter the magnetic deflection chamber was facilitated by horizontal and vertical electrical deflecting plates placed at the exit end of the kevatron, the magnetic field H_1, and adjustable pole pieces on the analyzer magnet which permitted changes in the height of the magnetic deflection chamber B. The procedure followed was to first align the apparatus for a beam of given energy, then to admit gas to the pipe A. The helium, air, and argon were admitted through a needle valve, and the hydrogen via a palladium leak.

After gas was admitted, the beam was magnetically separated into its charged states. A rough indication of the correct current in the magnet to deflect the charged beams into their ports was obtained by observing beam currents collected on the nickel sheaths of the detectors. The exact value of the magnetic current was determined by taking a curve of the resistance change of the thermistor *versus* current in the magnet. In all cases the maximum heating occurred for the same magnet setting that gave the maximum charge collection. That being the case, in the later stages of the experiment the magnet settings were determined only by the maximum ion collection. Since the largest hole in the differential pumping system was 2 mm and the width of the detector entrances were $2\frac{1}{2}$ mm, the slight fluctuations in the current supply to the magnet could be tolerated. The beam currents were of the order of 10^{-8} ampere, but no attempt was made to get precise values by eliminating effects due to secondary electrons.

After allowing at least fifteen minutes for the temperature of the thermistors to come to equilibrium, their resistances were measured by a Wheatstone bridge. The resistances were measured several times with at least five minutes elapsing between measurements. Also, as a check that the correct magnet current was being used, sets of readings were taken for the current displaced either side of the original value. After the data were obtained, the thermistors were allowed to cool by deflecting the beam away from the apparatus and the resistance values of the thermistors at equilibrium with no heating were recorded. The above procedure was repeated for at least one more gas pressure to be sure that sufficient gas was admitted to the pipe for the beam to come to charge equilibrium.

The currents collected by diaphragm D_2 and the sheath in the 30° port were observed while the data were being taken so as to give an indication of the variation of beam intensity of the kevatron. Small fluctuations of the beam intensity were averaged out by the long time constant of the detector thermistor and sheath.

IV. ANALYSIS OF THE DATA

In this experiment, it was necessary to compare the intensities of three different beams each composed of particles of differing charge. This led to the selection of detectors whose response depended on the kinetic energy of the particles, and thus the measurements of beam intensities were reduced to the measurement of temperature changes.

Since the nickel sheath almost completely surrounded the thermistor, the assumption was made that the thermistor was at the same temperature as the sheath at equilibrium. Also, the small size of the thermistor and its leads as compared with the sheath further made this assumption justified.

In comparing beam intensities, essentially two steps were necessary. First, the change in resistance had to be converted to a temperature change, and then the temperature change converted into some arbitrary measure of beam intensity. Since the measurements were made after the detectors reached equilibrium temperatures, the latter stage was necessary since heat

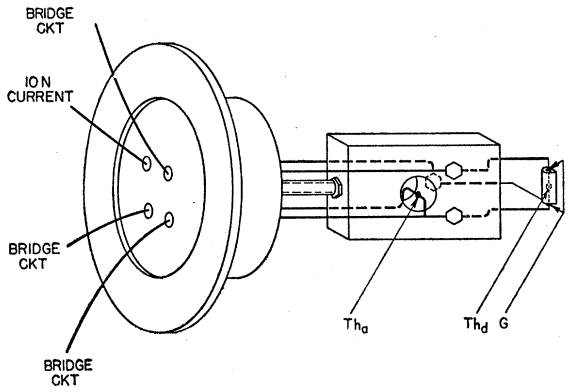

FIG. 2. Schematic drawing of the detector element, showing the beam-measuring thermistor Th_d and the thermistor for recording the ambient temperature Th_a.

TABLE I. Temperature *vs* resistance characteristics for the thermistor in the neutral (0° port) detector.[a]

R(ohms)	T(°C)
2175	15
1795	20
1495	25
1255	30
1060	35
899	40
768	45
658	50
506	55
490	60
425	65
372	70
326	75
287	80

[a] Notation: $R=R_0\exp[B(1/T-1/T_0)]$; $B=3183$ (1/°K); R=the resistance at temperature T; R_0=the resistance at temperature T_0. For temperature changes less than 10°C the following is a good approximate formula:

$$T-T_0=\Delta T\cong-\frac{T_0^2}{B}\frac{\Delta R}{R_0}\left\{1+\left(\frac{1}{2}+\frac{1}{4}\frac{T_0}{B}\right)\frac{\Delta R}{R_0}\right\}.$$

was lost both by metallic conduction along the leads, and radiation from the nickel sheaths. The pressure in the deflection chamber was low enough so that gaseous conduction could be neglected.

The 27A thermistor is a solid semiconductor with a resistance of approximately 2000 ohms at 25°C and with a temperature coefficient of resistance at 25°C of about −0.034 ohms/ohm °C. The temperature is related to the resistance by the formula

$$R=R_0\exp[B(T^{-1}-T_0^{-1})], \tag{1}$$

where R is the resistance at temperature T, R_0 the resistance at temperature T_0, and B is a parameter depending on the materials from which the thermistor is made. For the limited temperature range of 0°C to 150°C, for which the 27A thermistor is designed, B is a constant and equal to 3183. A calibration curve was obtained by a temperature bath for temperatures from 13°C to 63°C. As would be expected from Eq. (1), when $\log R$ is plotted against $1/T$, the points fall on a straight line. The slope of this line was the same to within 2 percent for all six thermistors used and the rated values given by Western Electric. The resistance values at 25°C varied from 1450 to 1800 ohms as compared with the typical characteristics given by Western Electric of 2000 ohms±25 percent.

In converting from resistance to temperature, temperature changes larger than 5°C were obtained from the calibration curves. For temperature changes ΔT, less than 5°C, R in Eq. (1) was expanded in powers of ΔT, and terms beyond $(\Delta T)^2$ were dropped. This approximate equation, when solved for ΔT, gives

$$\Delta T\cong-\frac{T_0^2}{B}\frac{\Delta R}{R_0}\left\{1+\left(\frac{1}{2}+\frac{1}{4}\frac{T_0}{B}\right)\frac{\Delta R}{R_0}\right\}.$$

Temperature T_0 was obtained from the calibration curve for the thermistor used to measure the ambient temperature.

At equilibrium, the relation between beam intensity and temperature change is determined by the incoming heat being equal to the heat carried away by metallic conduction along the leads and radiation from the surface of the nickel sheath. At equilibrium, the incident power Q and the temperature change $\Delta T=T_d-T_a$, are related by the formula $Q=\alpha(\Delta T)+\beta(T_d^4-T_a^4)$, or

$$Q=[\alpha+4\beta T_a^3]\Delta T+6\beta T_a^2(\Delta T)^2+4\beta T_a(\Delta T)^3+\beta(\Delta T)^4, \tag{2}$$

where $\alpha(\Delta T)$ is the heat lost by metallic conduction and $\beta(T_d^4-T_a^4)$ the net heat lost by radiation. T_d and T_a are the detector and ambient temperatures, respectively. Q is a nonlinear function of ΔT, which for small temperature changes can be approximated by

$$Q=[\alpha+4\beta T_a^3](\Delta T). \tag{3}$$

To compare the temperature changes of the three detectors in order to get the fractions of the total beam in each of the charge states, an equivalent temperature change ΔT_e was obtained, which when substituted into Eq. (3) gave the same value for Q as would be obtained from substituting the measured temperature change ΔT into Eq. (2). By making the geometry of the detectors the same, α and β had the same values for the three detectors. If then, as was the case, the three detectors had the same ambient temperature T_a, the ratios of the beam intensities would be equal to the ratios of the ΔT_e's. If the two expressions for Q are equated and the resulting equation solved for ΔT_e, ΔT_e is expressed as a function of ΔT:

$$\Delta T_e=\Delta T+\frac{1}{(\alpha/\beta)+4T_a^3}[6T_a^2(\Delta T)^2+4T_a(\Delta T)^3+(\Delta T)^4]. \tag{3'}$$

When the temperature change ΔT is small, $\Delta T_e=\Delta T$ is a good approximation. For large ΔT the term in brackets must also be considered. The only unknown quantity on the right-hand side of Eq. (3′) is α/β. To obtain a curve of ΔT_e *versus* ΔT for a given value of T_a, sets of data were taken for large and for small temperature changes by varying the beam intensity from the kevatron for constant voltage. In this way, the physical quantities which were to be determined served to calibrate the detectors.

Table I gives the resistance-temperature characteristic of one of the thermistors used, and Table II gives the calibration for temperature change *versus* beam intensity for an ambient temperature of 300°K. Table III gives a typical set of data and results.

V. DESCRIPTION OF CAPTURE AND LOSS IN TERMS OF CROSS SECTIONS

Although the cross sections for electron capture and loss are functions of the velocity, the cross sections

are so large throughout the energy range of these experiments that gas pressures in the pipe sufficient to produce charge equilibrium in the emergent beam were low enough so that no appreciable diminution in beam energy took place. Thus in setting up equations to describe the approach to equilibrium in the pipe, we can treat the cross sections as independent of the velocity.

Let N_0, N_1, N_2 be, respectively, the numbers of He^0, He^+, and He^{++} ions in the beam. The cross sections σ_{ij} are defined by the first index referring to the initial charge state of the particle and the second to the charge state resulting from interaction with the medium, for example, σ_{01} is the cross section for He^0 to lose an electron and become He^+. The differential equations to be solved are

$$\begin{aligned} dN_0/dp &= -(L/kT)[(\sigma_{01}+\sigma_{02})N_0-\sigma_{10}N_1-\sigma_{20}N_2], \\ dN_1/dp &= -(L/kT)[-\sigma_{01}N_0 \\ &\qquad +(\sigma_{10}+\sigma_{12})N_1-\sigma_{21}N_2], \\ dN_2/dp &= -(L/kT)[-\sigma_{02}N_0 \\ &\qquad -\sigma_{12}N_1+(\sigma_{20}+\sigma_{21})N_2], \end{aligned} \tag{4}$$

subject to the condition

$$N_0+N_1+N_2=N_t=\text{const}, \tag{5}$$

where N_t is the total number of particles in the beam, p is the pressure, L the length of the pipe (74.0 cm), k the Boltzmann constant, and T the absolute temperature. The cross sections σ_{02} and σ_{20} refer to the capture or loss of two electrons in a single encounter. The equilibrium conditions may be found by setting the pressure derivatives equal to zero. Thus one obtains

$$\begin{aligned} \left.\frac{N_0}{N_1}\right|_{\text{equil}} &= \frac{\sigma_{10}\sigma_{21}+\sigma_{20}(\sigma_{12}+\sigma_{10})}{\sigma_{01}\sigma_{21}+\sigma_{21}\sigma_{02}+\sigma_{20}\sigma_{01}} \doteq \frac{\sigma_{10}}{\sigma_{01}}, \\ \left.\frac{N_2}{N_1}\right|_{\text{equil}} &= \frac{\sigma_{01}\sigma_{12}+\sigma_{02}(\sigma_{12}+\sigma_{10})}{\sigma_{21}\sigma_{01}+\sigma_{21}\sigma_{02}+\sigma_{20}\sigma_{01}} \doteq \frac{\sigma_{12}}{\sigma_{21}}, \end{aligned} \tag{6}$$

TABLE II. Conversion of temperature change to beam intensity for $T_a=300°K$.[a]

ΔT(°C)	ΔT_e
0	0
5	5.1
10	10.3
15	15.8
20	21.4
25	27.2
30	33.2
35	39.4
40	45.9
45	52.4
50	59.3
55	66.4
60	73.7
65	81.2
70	89.1

[a] Notation: T_d = the temperature of the detector; T_a = the ambient temperature; $\Delta T = T_d - T_a$; Q = incident power in beam; at equilibrium $Q = \alpha(\Delta T) + \beta(T_d^4 - T_a^4) = [\alpha + 4\beta T_a^3]\Delta T + 6\beta T_a(\Delta T)^2 + 4\beta T_a(\Delta T)^3 + \beta(\Delta T)^4$; $\alpha(\Delta T)$ = heat lost per second by metallic conduction along the leads; $\beta(T_d^4 - T_a^4)$ = heat lost per second by radiation from the surface of the nickel sheath; ΔT_e = temperature change such that $Q = [\alpha + 4\beta T_a^3]\Delta T_e$.

TABLE III. Typical set of data and results.[a] Beam energy = 400 kev.

Port	R_d	R_a	T_d	T_a	ΔT	ΔT_e	F_i
0°	871	1440	41.0	26.5	14.5	15.4	0.168
30°	274	1311	80.6	28.9	51.7	64.9	0.708
60°	1173	1560	39.0	28.3	10.7	11.3	0.123

[a] Notation: He^0 was detected in the 0° port; He^+ was detected in the 30° port; He^{++} was detected in the 60° port; R_d = the resistance in ohms of the detector thermistor; R_a = the resistance of the thermistor used to measure the ambient temperature; T_d = the temperature in °C of the detector thermistor; T_a = the ambient temperature; $\Delta T = T_d - T_a$; ΔT_e = the equivalent temperature change such that the incident power is proportional to ΔT_e (see Table II); F_i = the fraction of the total beam in the various charge states (He^0, He^+, He^{++}).

in which the simpler expressions at the right assume that the double electron cross sections are small compared to the others.

Although the primary purpose of this research was to obtain the equilibrium ratios, it was necessary to ascertain that sufficient gas had been admitted to the pipe to produce equilibrium, and in such tests a few measurements were made in which the change of the emergent beam from the pure He^+ from the kevatron to the final equilibrium mixture was followed as a function of pressure. The expressions for the initial rates of change of the numbers N_0, N_1, and N_2 may easily be found by imposing the conditions $N_0=N_2=0$ and $N_1=N_t$ on the original differential equations. Thus one obtains the initial pressure variations,

$$\begin{aligned} N_0/N_t &= (L/kT)\sigma_{10}p, \\ N_1/N_t &= 1-(L/kT)(\sigma_{10}+\sigma_{12})p, \\ N_2/N_t &= (L/kT)\sigma_{12}p. \end{aligned} \tag{7}$$

In the next section these equations will be used to obtain approximate values of the cross sections for two beam energies.

VI. RESULTS AND ERRORS

The results on the equilibrium distributions for the charge states of a helium beam after passing through hydrogen, helium, air, and argon are given in Figs. 3 and 4. Table IV gives the fractions of the total beam in each of the charge states in 20-kev steps. The values were obtained from the smooth curves drawn through the experimentally determined points. Table V is a summary of some of the features which facilitate a comparison of the data taken on the four gases.

The helium used was 99.8 percent pure with the remaining 0.2 percent hydrogen; it was obtained from the National Cylinder Gas Company. The hydrogen was admitted through a palladium leak which served the double purpose of being a valve and purifying the hydrogen. The argon was 99.9 percent pure and prepared by the Matheson Company. The air was dried and freed of CO_2 by passing the air from the laboratory through KOH, "Dryerite," and glass beads dusted with P_2O_5.

The objective of this research was to obtain the equilibrium ratios, leaving the problem of finding the

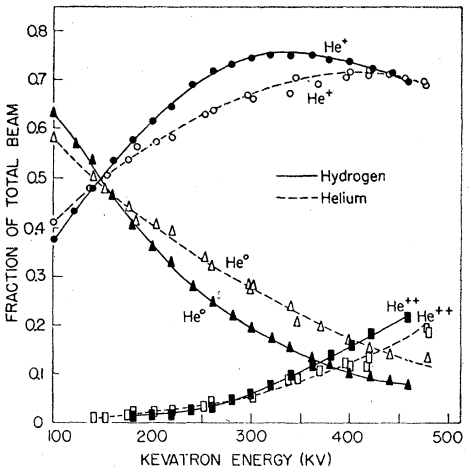

FIG. 3. Charge distribution as a function of energy for a helium beam in hydrogen and helium.

individual cross sections for a later effort. However, some rough estimates of the cross sections can be made from the data. The distribution of the beam in its charge states as a function of pressure was measured at 131 kev and 340 kev for helium as the target gas. By using Eqs. (7) for the initial change in charge as a function of pressure, rough estimates of the cross sections σ_{10} and σ_{12} can be obtained. Then, σ_{01} and σ_{21} can be determined by Eqs. (6) and the curves for helium. At 131 kev the values found are $\sigma_{01}=\sigma_{10}=1.72\times10^{-16}$ cm$^2\pm30$ percent. N_2 was small enough at this low energy so that it could be neglected. At 340 kev, the values of the cross sections found were $\sigma_{01}=8.3\times10^{-17}$ cm^2, $\sigma_{10}=3.1\times10^{-17}$ cm^2, $\sigma_{12}=1.4\times10^{-17}$ cm^2, and $\sigma_{21}=1.2\times10^{-16}$ cm^2. These values are correct to within 20 percent. Figure 5 shows the pressure variation at 340 kev.

As a check that all of the He^{++} beam was collected, the ratio of the intensities of the He^{++} and He^0 beams was measured by deflecting the He^{++} into the 30° port. The ratio so obtained agreed to within 2 percent of the value obtained in the usual way by having the He^{++} beam enter the 60° port. This check was made for helium gas and at 460 kev, where the He^{++} and He^0 beam intensities are comparable in magnitude. Also, for air at 130 kev the He^+ beam was detected by deflection into the 60° port. The He^+ to He^0 ratio was within 3 percent of the value obtained by He^+ detection in the 30° port. These checks also established that the 30° and 60° detectors were, in fact, equal in their response to the same beam.

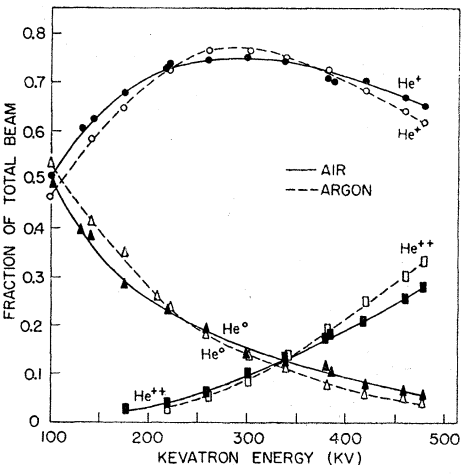

FIG. 4. Charge distribution of a helium beam as a function of energy in air and argon.

The errors in this experiment result mainly from the fluctuations in the kevatron beam. The errors can best be estimated by seeing how closely the points fall on a smooth curve. Each point represents the average of at least four sets of data and gives the results of one run. In the energy range from 200 kev to 400 kev, the error in the fraction of He^+ probably did not exceed 2 percent. Below 200 kev, the error in the He^+ beam was probably as high as 5 percent. This is due to the smaller beam intensities available at these lower energies. Above 400 kev, the beam fluctuations became more pronounced which probably resulted in an error in the He^+ beam of about 5 percent.

The beam energy was measured correctly to within 1 kev for energies up to 400 kev and to within 2 kev above 400 kev. The larger error at high energies was due to slight variations in the energy of the beam resulting from the beam fluctuations which affected the loading on the kevatron. The measurements of the resistances of the thermistors and their conversion into temperatures was correct to within 0.1°C for temperatures less than 10°C and for higher temperatures probably did not exceed 0.3°C.

VII. DISCUSSION

By Eqs. (6) the ratios of the capture and loss cross sections between He^0 and He^+, and between He^+ and He^{++} can be obtained from the equilibrium beam intensities, provided the assumption is made that the double captures and losses are negligible. Since the various theoretical calculations of the cross sections are based on approximations which lead to a power dependence on the energy, in Fig. 6, $\log(N_1/N_0)$ and $\log(N_2/N_1)$ are plotted *versus* log$E$. Bohr[16] indicates that the loss cross section σ_l should be proportional to $1/V^n$, where n is a function of the atomic number Z of the material being traversed and the velocity of the particle, and varies from 0 to 2. n decreases with increasing Z and decreases for V less than $V_0=e^2/\hbar$, the velocity of an electron in the first Bohr orbit. By the Born approximation, Brinkman and Kramers[17] found

[16] N. Bohr, Kgl. Danske Videnskab. Selskab, Mat.-fys. Medd. **18**, No. 8 (1948).

[17] H. C. Brinkman and H. A. Kramers, Proc. Akad. Amsterdam **33**, 973 (1930).

TABLE IV. Charge distribution for a helium beam in hydrogen, helium, dry air, and argon.[a]

Energy (kv)	Hydrogen F_0	Hydrogen F_1	Hydrogen F_2	Helium F_0	Helium F_1	Helium F_2	Dry air F_0	Dry air F_1	Dry air F_2	Argon F_0	Argon F_1	Argon F_2
100	0.63	0.37	···	0.59	0.41	···	0.50	0.50	···	0.53	0.47	···
120	0.57	0.43	···	0.54	0.45	···	0.43	0.57	···	0.48	0.52	···
140	0.52	0.48	···	0.51	0.48	0.01	0.38	0.62	···	0.42	0.58	···
160	0.47	0.53	···	0.47	0.52	0.015	0.34	0.66	···	0.37	0.63	···
180	0.41	0.57	0.015	0.43	0.55	0.02	0.28	0.69	0.025	0.33	0.67	···
200	0 36	0 62	0.02	0.40	0.57	0.025	0.26	0.71	0.03	0.28	0.70	0.02
220	0.32	0.66	0.025	0.38	0.59	0.03	0.23	0.73	0.035	0.24	0.73	0.03
240	0.28	0.69	0.03	0.35	0.61	0 035	0 21	0 74	0.05	0.21	0.75	0.04
260	0.25	0.72	0.035	0.32	0.63	0.04	0.19	0.75	0.065	0.18	0.77	0.055
280	0.22	0.73	0.05	0.30	0.65	0.05	0.17	0.75	0.08	0.16	0.77	0.07
300	0.19	0.75	0.06	0.28	0.67	0.06	0.15	0.76	0.095	0.15	0.77	0.085
320	0.17	0.75	0.075	0.25	0.68	0.07	0.14	0.75	0.11	0.13	0.76	0.11
340	0.15	0.76	0.095	0.23	0.69	0.085	0.13	0.74	0.13	0.11	0.75	0.13
360	0.13	0.75	0.12	0.21	0.70	0.095	0.12	0.73	0.15	0.095	0.74	0.16
380	0.12	0.74	0.14	0.19	0.71	0.11	0.11	0.72	0.17	0.085	0.73	0.19
400	0.10	0.74	0.16	0.17	0.71	0.12	0.095	0.71	0.19	0.07	0.71	0.22
420	0.095	0.73	0.18	0.16	0.71	0.13	0.08	0.70	0.21	0.06	0.69	0.25
440	0.085	0.72	0.20	0.14	0.71	0.15	0.07	0.69	0.24	0.055	0.66	0.28
460	0.08	0.70	0.22	0.13	0.70	0.17	0.065	0.68	0.26	0.05	0.64	0.30
480	···	···	···	0.11	0.68	0.20	0.055	0.66	0.29	0.045	0.62	0.33

[a] Notation: F_0 equals the fraction of He^0 in the beam; F_1 equals the fraction of He^+ in the beam; F_2 equals the fraction of He^{++} in the beam.

that the capture cross section σ_c was proportional to $1/V^{12}$, for $V \gg V_0$. Bohr[16] got a $1/V^6$ dependence for σ_c when $V > V_0$ and for material of large Z, by statistical considerations based on the assumption that the electron captured was one which in the substance had a velocity approximately equal to the velocity V of the particle. For velocities less than V_0 it would be expected that σ_c would be less sensitive to velocity, for σ_c cannot become significantly greater than the geometrical cross section. The above considerations indicate that σ_l/σ_c is proportional to V^m, where m increases with increasing V, and increases with increasing atomic number for Z large enough to make Bohr's statistical considerations valid ($Z > 5$).

Table VI gives the values of m for the gases studied.

In the energy range considered, m is a constant for exchange between He^+ and He^{++}. For exchange between He^0 and He^+ all the curves show the increase of m with velocity. The values of m for air and argon show the expected dependence on Z. Not very much can be said about the values of m for helium and hydrogen; the Bohr $1/V^6$ dependence breaks down because of the low atomic number, and Brinkman and Kramers' $1/V^{12}$ dependence does not apply because of the low value of V/V_0.

The energies at which $N_0 = N_1$ and $N_1 = N_2$ are of interest because they represent the energies at which $\sigma_{01} = \sigma_{10}$ and $\sigma_{12} = \sigma_{21}$. For proton beams the energy E_{01}, at which the capture and loss cross sections are equal corresponds to a velocity V_{01} of the proton,

TABLE V. Summary of data.[a]

	E_{01}	E_{02}	$(F_1)_{max}$	$(E_1)_{max}$	F_{02}
Hydrogen	148 kev	370 kev	0.76	340 kev	0.13
Helium	145	430	0.72	410	0.15
Air	98	340	0.76	300	0.13
Argon	115	330	0.77	290	0.12

[a] Notation: F_0 = fraction of He^0 in the beam; F_1 = fraction of He^+ in the beam; F_2 = fraction of He^{++} in the beam; E_{01} = energy at which $F_0 = F_1$; E_{02} = energy at which $F_0 = F_2$; $(F_1)_{max}$ = maximum value of F_1; $(E_1)_{max}$ = energy at which $F_1 = (F_1)_{max}$; F_{02} = the value of F_0 when $F_0 = F_2$.

TABLE VI. Values of the exponent m in the power dependence of σ_l/σ_c on V.[a]

	Charge exchange between He^0 and He^+				Charge exchange between He^+ and He^{++}	
	E_{01}	V_{01}/V_0	m at 100 kev	m at 450 kev	E_{12}	m
Hydrogen	148 kev	1.22	2.6	4.0	660 kev	6.1
Helium	145	1.21	2.0	4.0	800	5.1
Air	98	0.99	2.8	4.3	650	5.2
Argon	115	1.08	3.4	5.1	580	6.3

[a] Notation: E_{01} = energy at which the He^0 and He^+ equilibrium beams are equal; E_{12} = energy at which the He^+ and He^{++} equilibrium beams are equal; V_{01} = the velocity of helium at which it has the energy E_{01}; $V_0 = e^2/\hbar$, the velocity of an electron in the first Bohr orbit. For helium V_0 corresponds to the energy $E_0 = 99.2$ kev; m = the exponent of the power dependence of σ_l/σ_c on V ($\sigma_l/\sigma_c \propto V^m$).

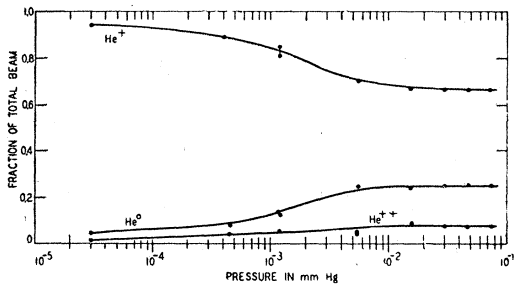

FIG. 5. Charge distribution as a function of pressure for a 340-kev helium beam emerging from a 74-cm long tube containing helium gas. The incident beam is all He^+.

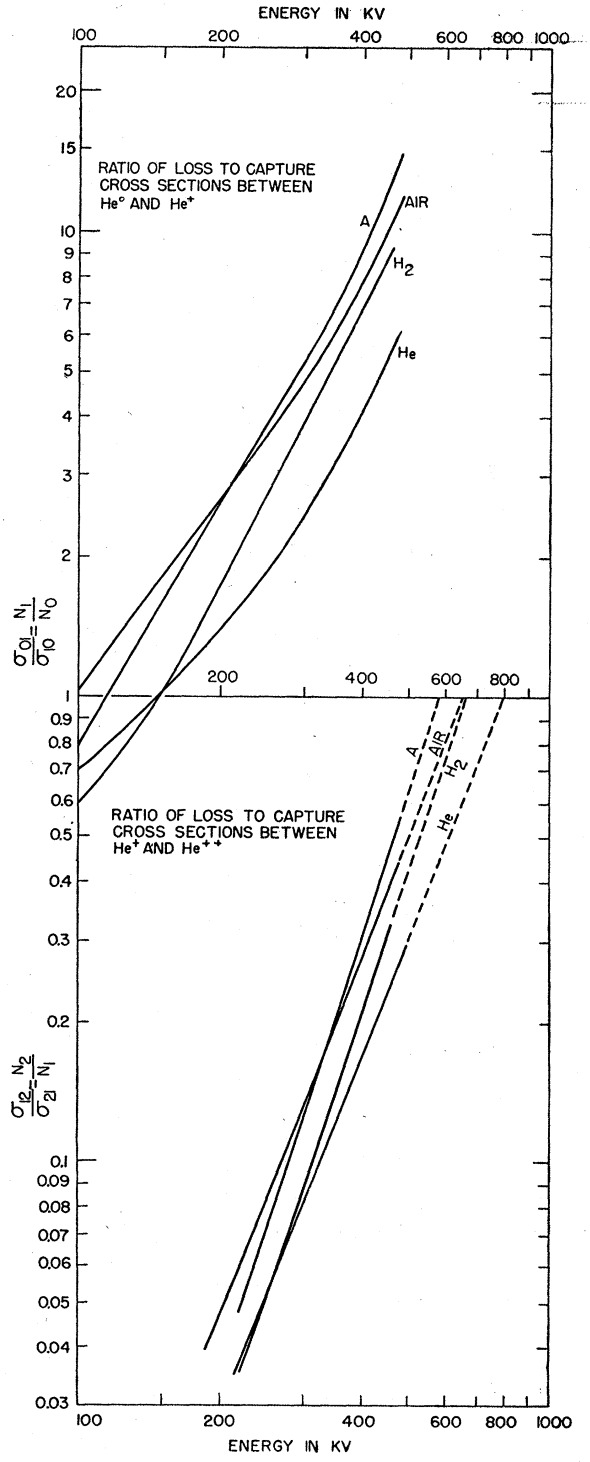

FIG. 6. The ratio of the loss to capture cross sections plotted as a function of beam energy.

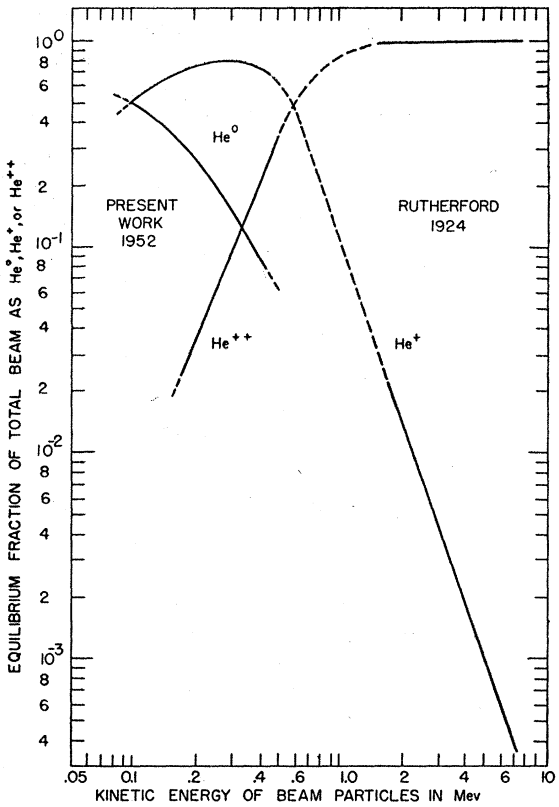

FIG. 7. Equilibrium charge distribution from 100 kev to 6 Mev for a helium beam traversing air.

approximately equal to V_0. For hydrogen beams in metals Hall[6] found $V_{01}=0.95V_0$, Montague and Ribe[8] got $V_{01}=1.44V_0$ for protons in hydrogen, and Kanner[9] got $V_{01}=1.0V_0$ for protons in air. Table VI gives V_{01}/V_0 for the present work. The agreement between the values of V_{01}/V_0 for hydrogen and helium beams in air is striking.

Table VI also gives the values of the energy E_{12} at which the capture and loss cross sections between He^+ and He^{++} are equal. These values were obtained by extrapolation (indicated by dashed lines in Fig. 6). The work by Rutherford[3] for a helium beam in air gave a value of $E_{12}=646$ kev, as compared with the value here obtained of $E_{12}=650\pm20$ kev.

Figure 7 gives the charge distribution as a function of energy for the present work and the data obtained by Rutherford, for a helium beam in air.

The author wishes to express his gratitude to Professor S. K. Allison who suggested the problem and extended the facilities of his laboratory for its solution. Mr. Gordon DuFloth was of great assistance in maintaining the equipment and taking data.